SATELLITE DETECTION OF VEGETATION CHANGE IN Northeast North America from 2000 to 2016

Kristen Thiebault
Salem State University

Stephen Young
Salem State University

ABSTRACT

This research used the Moderate-Resolution Imaging Spectroradiometer (MODIS) MOD13C2 Normalized Difference Vegetation Index (NDVI) and MOD11C3 Land Surface Temperature (LST) data to analyze changes in photosynthesis for northeastern North America from 2000 to 2016. The Northeastern states of New York, Connecticut, Rhode Island, Massachusetts, Vermont, New Hampshire, and Maine along with the Canadian provinces of Newfoundland and Labrador, Quebec, New Brunswick, Nova Scotia, and Prince Edward Island were analyzed for changes at the seasonal and annual scales. The methods of univariate differencing and the time series Mann-Kendall significance test were used to analyze change. During this period, levels of photosynthesis increased throughout much of the region at the annual and seasonal scales. Increasing NDVI was the least in the spring and the greatest in the summer. Very few areas decreased in NDVI during this time-period. This research also analyzed how the eight most extensive land covers of the region changed, with high latitude open shrub lands and lower latitude mixed forest increasing the most. Related to this change was an increase in LST, with much of the region increasing in temperature greater than 0.5° C. Over 80 percent of the region increased greater than 0.5° C during the summer. There was not, however, a direct relationship between changes in NDVI and changes in LST, as increasing vegetation tends to decrease LST. This paper presents the regions of vegetation change and the intensity of vegetation change in the study area.

Introduction

Changes in the phenology and distribution of plants and animals are occurring globally in all well-studied terrestrial, marine, and freshwater ecosystems (Parmesan 2006). These observed changes are primarily occurring due to a warming world (Chen et al. 2011). The high northern latitudes have experienced greater warming than other regions of the world in recent decades and evidence from marine, terrestrial and atmospheric studies show that the climate of this region has warmed significantly in the last thirty years (Serreze and Francis 2006). The rate of change in the Arctic is now faster than ecosystems can adapt to naturally (Wassman et al. 2011). The northern high latitudes are undergoing a system-wide response to an altered climatic state and warming has led to changes in this region's vegetation composition, density, and distribution (Tape, Sturm and Racine 2006; Elmendorf et al. 2012). It is highly likely that these changes will intensify in the coming decades as the climate continues to warm. Various field experiments have shown that northern ecosystems have responded to warming and precipitation changes in a variety of ways (Chen et al. 2006; Peng et al, 2011), however, the extension of these findings to the larger pan-Northern region is constrained by the limited number of studies (Yi et al. 2013).

There are numerous reasons to be worried about a warming and changing Boreal to Arctic region. The snow and ice that covers much of the Arctic region (permanent and seasonal) has a strong influence on the Earth's energy balance by reflecting incoming solar radiation back to space. With declining snow and ice (Schlaepfer, Lavenroth and Bradford 2012) less of this energy is being returned to space, contributing to terrestrial warmth. Northern Boreal and Arctic ecosystems are also a land sink for atmospheric CO_2 (McGuire et al. 2009), and large quantities of organic carbon and methane are stored in frozen soils (permafrost) within Arctic and sub-Arctic regions (Schuur et al. 2015). With the melting of the permafrost, carbon and methane are being released into the atmosphere, adding to the greenhouse effect. The Arctic region has the greatest concentration of potential tipping elements in the Earth's system (Duarte et al. 2012).

Tools for better understanding our shifting world include the use of remote sensing to make observations of how our world is changing (Young 2004; Hansen and Sato 2012; Hansen et al. 2013; Ren et al. 2015). With satellite remote sensing, we can detect a wide range of land parameters, such as biomass and productivity that can serve as critical inputs for climate models as well as mapping the surface of the biosphere (Young and Harris 2005; Zhang et al. 2008; Kimball et al. 2009). Remote sensing also allows us to see the state of the Earth at specific times in a repeatable manner, which helps us understand the drivers of change (Hansen et al. 2013). Regional and global monitoring with satellite data can also detect changing vegetation and growing conditions; (Mildrexler et al. 2007; Yi et al. 2013 Wang et al. 2016). The most widely used satellite-derived vegetation index for vegetation change analysis is the Normalized Difference Vegetation Index (NDVI), providing a tested surrogate for the amount of green foliage (Xie, Sha, and Yu 2008; Fraser et al. 2011).

By using long-term satellite data, it has been discovered that in the northern high latitudes, the growing season is lengthening, and this has led to enhanced productivity (Tape, Sturm and Racine 2006; Chen et al. 2006). The pan-Arctic increased greening was found to correlate with increasing temperatures (Zhang et al. 2004; Bhatt et al. 2010). Warmer spring temperature will generally enhance vegetation productivity by extending the growing season (Menzal et al. 2006). Using 1 km resolution Advanced Very High-Resolution Radiometer (AVHRR) satellite data, Pouliot, Latifovic and Olthof (2009) found 22 percent of the vegetated area in Canada between 1985 and 2006 had a positive NDVI trend based on the Mann–Kendall test at the 95 percent confidence level. Concerning northeast North America, Fraser et al. (2011) used Landsat (30-meter resolution) data to analyze vegetation trends in Northern Canada at four national parks. One of the parks, located in the northeast Torngat Mountains National Park in

Labrador, was found to be increasing in NDVI from 1985 to 2009. They discovered that the major change in land cover was a replacement of bare cover by shrub in the broad valleys and by herbaceous vegetation on the lower hillslopes. Ju and Masek (2016) used peak-summer Landsat surface reflectance data from 1984–2012 to measure changes in NDVI across Canada and Alaska. They found that the most intensive and extensive greening occurred in northern Quebec and northern Labrador during this period. They found both some browning and greening of the boreal forests of Quebec.

While increases in air temperature in the high latitudes is increasing NDVI, Kaufmann et al. (2003) have found temperature-induced increases in vegetation might have actually slowed increases in surface temperature. This increase in vegetation growth might be offsetting a portion of anthropogenic warming. While the reductions in the extent of snow cover increases land surface temperature, it appears that increases in vegetation within land covers reduce temperature. Many urban heat island studies have also established the correlation between increases in green areas and a reduction in local urban temperatures (Kafatos 2007; Takebayashi and Moriyama 2007).

The objective of this research is to build upon these earlier studies by analyzing and mapping changes in photosynthesis for northeastern North America (Figure 1) using satellite-derived NDVI data as a proxy for photosynthesis. In the process of accomplishing this we: 1) measured the significance, intensity and location of change in NDVI between 2000 and 2016, 2) determined how different land cover types changed in NDVI, and 3) investigated the relationship between changes in vegetation and land surface temperature (LST).

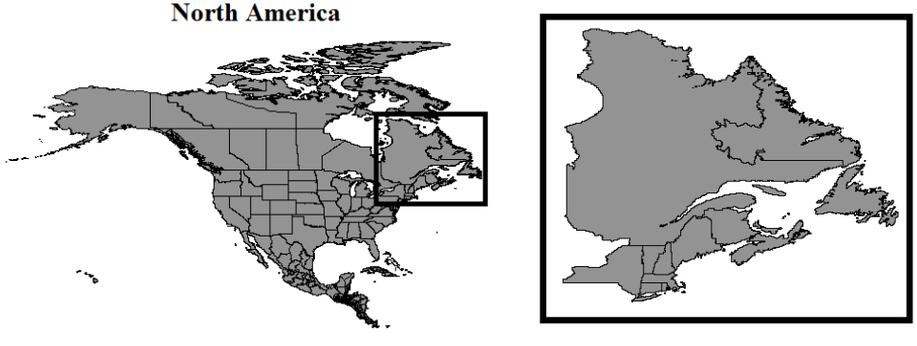

Figure 1. Map of study area.

Data

All satellite data used in this study came from the Moderate-Resolution Imaging Spectroradiometer (MODIS) sensor on-board the National Aeronautics and Space Administration's (NASA) Terra satellite. Terra overpasses the equator at around 10:30 A.M. (10:30 P.M.) local

time. The data were downloaded from NASA's Earth Observing System Data and Information System (EOSDIS) via the Reverb portal (http://reverb.echo.nasa.gov/reverb/). Data from February 2000 to December 2016 for two MODIS data sets, MOD11C3 and MOD13C2 were downloaded. Additionally, the MODIS-derived land cover product, MCD12C1 was downloaded for the year 2005.

MOD11C3 Data

The MODIS/Terra Land Surface Temperature and Emissivity Monthly L3 Global 0.05 Degree Climate Modeling Grid (CMG), Version 6 (MOD11C3) data were used to map Land Surface Temperature (LST) in this study. The MOD11C3 is a CMG product at a 0.05° resolution (about 5.6 km) with global coverage and includes both night and day LST layers. Monthly LST and emissivity values are derived from compositing and averaging the values from the corresponding month's MOD11C1 daily files (Wan, 2013, 2014). The MOD11 series temperature data have been widely used to measure and analyze LST (Gaddam et al. 2016; Yu et al. 2014).

MOD13C2 Data

The MODIS/Terra Vegetation Index (VI) Monthly L3 Global 0.05 Degree Climate Modeling Grid (CMG), Version 6 (MOD13C2) Normalized Difference Vegetation Index (NDVI) data were used in this study. The MOD13C2 is a CMG product at a 0.05° resolution (about 5.6 km) with global coverage. NDVI products derived from MODIS are based on a band ratio of MODIS band 1 (red) (0.620-0.670μm) and band 6 (near-infrared) (1.628-1.652μm). These bands are used to calculate the NDVI, defined as:

$$\text{NDVI} = \frac{\text{band 6} - \text{band 1}}{\text{band 6} + \text{band 1}}$$

The output values range from -1 to 1. The global MOD13C2 data are cloud-free temporal composites of the 16-day MOD13C1 product (Didan 2015). Cloud-free coverage is accomplished by replacing clouds with historical MODIS time series climatology record in the input data from the 16-day MOD13C1 product (Didan et al. 2015). The 16-day files were then averaged into monthly composites. The MOD13 Version 6 series provides consistent spatial and temporal time series for the comparison of vegetation at the global scale (Didan et al. 2015). The MOD13 series has been widely used for vegetation change analysis (Detsch, et al. 2016; Bastos, 2017; Kumar and Jeganathan, 2017).

MCD12C1

The Land Cover Type Climate Modeling Grid (CMG) product (MCD12C1) is a global land cover map with a spatial resolution 0.05° (about 5.6 km) derived from MODIS data. The land-cover types used in the product are the 17 land-cover classes following the International Geosphere–Biosphere Program (IGBP) scheme (Friedl et al. 2010). The MCD12C1 land cover data set has been used widely in vegetation analysis studies (Jimenez-Munoz et al. 2012; Andela and Van Der Werf, 2014). We used the land cover data for 2005, land covers near the beginning of the research period.

Data Compositing

MOD13C2 and MOD11C3 were composited into annual and seasonal data sets. For annual composites, all 12 months in the calendar year were added together and divided by 12. For seasonal data: Spring = (March + April + May)/3; Summer = (June + July + August)/3; and Fall = (September + October + November)/3. As there is no data for January and February of 2000 (the Terra MODIS sensor did not create usable data until late February 2000), January and February of 2001 are used in calculating the annual average for the year 2000.

Methods

Masking of Data

Data preparation and analyses was performed using the *Idrisi* image processing software from Clark Labs (https://clarkslabs.org/terrset/). All the data sets (MOD11C3, MOD13C2 and MCD12C1) were imported into *Idrisi*. Once imported, all imagery was windowed where water and land outside of the study area were masked out. The study area consists of the northeastern states of New York, Connecticut, Rhode Island, Massachusetts, Vermont, New Hampshire and Maine along with the Canadian provinces of Newfoundland and Labrador, Quebec, New Brunswick, Nova Scotia, and Prince Edward Island.

Profiling Data

Temporal profiles of the NDVI and LST data were generated for the annual and the seasonal data with results being graphed in excel. For each year, the value of all the pixels in the region are averaged for annual and seasonal NDVI and LST and the averaged values were graphed for each year of the data. In addition, a three-year running average was created and displayed with the profiles. This process was performed to determine the general direction in which the entire region's NDVI and LST was moving (increasing, decreasing or stable) and the inter-annual variation throughout the entire time period.

Change Analysis – Univariate Differencing

Univariate Differencing is the subtraction of NDVI and LST values at the beginning of the time series from those values at the end of the time series. This is one way to determine change from the beginning of a time-period to the end (Singh, 1989). To reduce outlier years, five-year averages were created for the seasonal and annual data. The five-year averages for MOD11C3 and MOD13C2 data were [(2000+01+02+03+04)/5] and [(2012+13+14+15+16)/5]. Because of almost complete snow cover and low sun angles, a winter season for each data set was not analyzed. The annual data, however, includes the winter months. Using MOD11C3 and MOD13C2 data, to discover areas that display changes in LST and NDVI and to determine the amount of change, the difference (raw change) between seasonal and annual averages were calculated:

$$\text{Difference} = [(2012+13+14+15+16)/5] - [(2000+01+02+03+04)/5]$$

For each of the seasonal and annual analyses, MOD13C2 pixels of NDVI change fell into one of seven categories: greater than 0.1 NDVI decrease, 0.05 to 0.1 decrease, 0.025 to 0.05 decrease, 0.025 decrease to 0.025 increase (neutral), 0.025 to 0.05 increase 0.05 to 0.1, increase and greater than 0.1 increase. For each of the seasonal and annual analyses, MOD11C3 pixels of LST change fell into one of five categories: greater than 1° C decrease, 0.5 to 1° C decrease, between 0.5° C decrease to 0.5° C increase (neutral), 0.5 to 1° C increase, and greater than 1° C increase. For the NDVI data, a percent change in NDVI was also calculated by:

$$\text{Percent change} = \frac{[(2012+13+14+15+16)/5] - [(2000+01+02+03+04)/5]}{[(2000+01+02+03+04)/5]}$$

For each of the seasonal and annual analyses, pixels of percent change fell into one of seven categories: greater than 20 percent NDVI decrease, 10 to 20 percent decrease, 5 to 10 percent decrease, 5 percent decrease to 5 percent increase (neutral), 5 to 10 percent increase, 10 to 20 percent, increase and greater than 20 percent increase.

Change Analysis – Time Series Significance Tests

In addition to the univariate differencing, we performed a time series significance test using a Mann-Kendall statistic. We performed this analysis using the Earth Trends Modeler in the Idrisi imagine processing software (Neeti and Eastman, 2011). This time series analysis is done on a pixel-by-pixel base and determines for each pixel location if the trend of change is significant or not along with the intensity of the change. The Earth Trends Molder produces a pair of images with an intensity of change image, expressed as Z scores, and a second image that expresses the probability that the observed trend could not have occurred by chance, expressed as p-values.

We reclassed the p-value image into a gray-level threshold image where 0 = not significant and 1 = significant at the 95 percent confidence level. We then multiplied the reclassed significance image by the z-score image to show the intensity of the significant changes that have occurred in northeastern North America. The intensity image was then reclassified into seven classes; no significant change, <-3 standard deviations from the mean (SD), -3 to -2 SD, -2 to 0 SD, 0 to 2 SD, 2 to 3 SD, and >3 SD. This procedure was performed on both the NDVI and LST data.

We then compared the simple differencing methodology with the time series significance analysis by creating a 95 percent confidence mask. We then multiplied this mask by the simple differencing change images for the annual and seasonal scales. This was done to see how much of the simple differencing changes were actually significant.

To further understand where changes in NDVI were occurring, different land cover classes were analyzed at the annual and seasonal scales. The eight largest land covers within the study area were examined; open shrub lands, mixed forest, evergreen needleleaf forest, savannas, woody savannas, grasslands, cropland and natural vegetation mosaic, and deciduous broadleaf forest. Annual and seasonal NDVI p-value (above the 95 percent confidence level) and intensity images were masked eight times, leaving only one of the land covers each time. The percent

of significant (95 percent confidence level) pixels within each intensity class (i.e. 0 to 2 SD, 2 to 3 SD, etc.) was then calculated for each land cover type using the number of pixels in each intensity class, and the total number of pixels within the land cover type.

Results

MOD13C2 NDVI Raw Change, Percent Change, and Significant Change

Raw simple differencing changes in NDVI, over the period of 2000 to 2016, for the total study area showed some slight decrease in areas, but was dominated by neutral to moderate increases at the annual and for each of the seasons (Table 1, Figures 2 and 3). Based on the raw change in NDVI, the greatest amount of decreasing values (<- 0.025) occurred in the fall with 8 percent of the area declining in NDVI. All of the time-periods experienced at least a 45 percent increase (> 0.025) of NDVI with the spring experiencing the largest area of increase with 55.5 percent of northeastern North America increasing in NDVI (> 0.025).

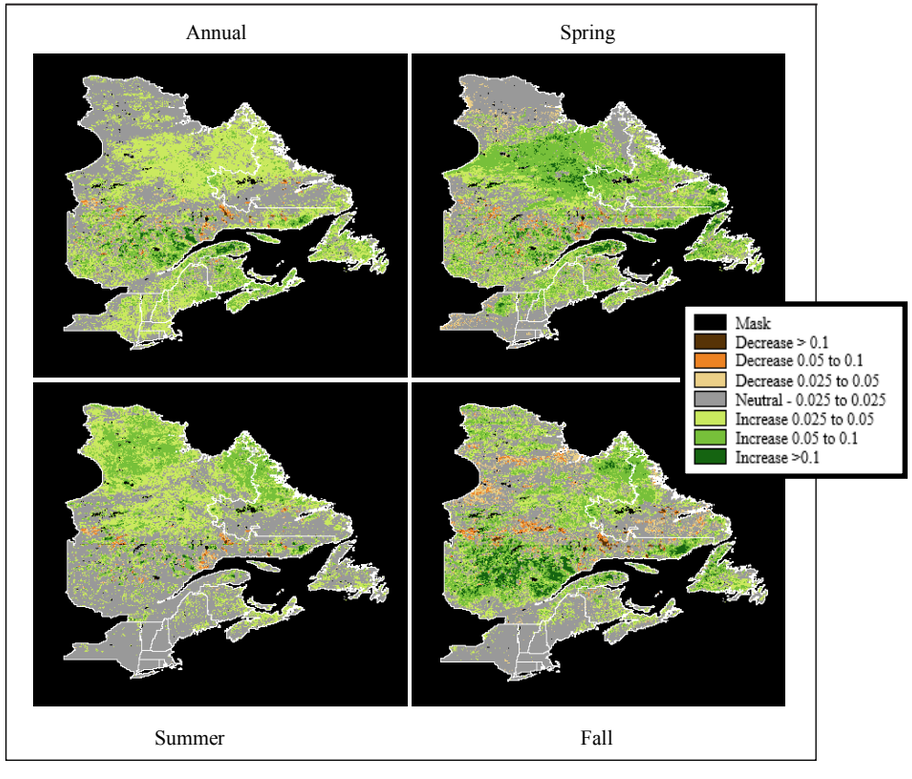

Figure 2. Raw NDVI Difference: Total Study Area.

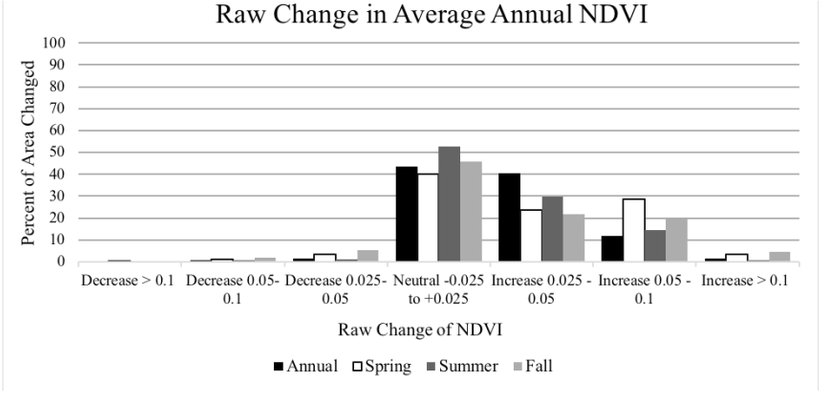

Figure 3. Changes in Raw NDVI: Total Study Area.

Concerning the percent change in NDVI (Table 2, Figures 4 and 5), during all of the time-periods there was a greater increase than decrease in NDVI. The spring had the greatest area of declining NDVI with 14 percent (> 5 percent decrease), but also had over 66 percent of the area increasing in NDVI (> 5 percent). In addition, the spring had the greatest area increasing in NDVI greater than 20 percent of NDVI for over 40 percent of the land area. All of the time-periods increased in NDVI (> 5 percent) with at least 36 percent of the area increasing.

While the raw and percent change analysis focused on differences between the beginning and end of the time-period, the time series significant tests analyzed change throughout the entire time-period. Concerning significant change at the 95 percent confidence level (Table 3, Figures 6 and 7) at the annual and seasonal levels, the greatest amount of decline was during the summer at 1.4 percent of the region while the smallest increase was during the spring at 10.95 percent of the region. The summer season saw the greatest increase, which was 47.87 percent of the entire study area. To determine the similarity between the areas of significant change (95 percent confidence level) and the simple differencing we determined how many of the simple differencing pixels were also pixels of significant change (Table 4). Here we found that most of the simple differencing pixels with an increasing NDVI greater than 0.1 were also areas of significant change (95 percent confidence level) for the entire time series. The annual scale had the highest

Percent Changes in Raw NDVI for study area				
Raw Change in NDVI	Annual	Spring	Summer	Fall
Decrease > 0.1	0.16	0.17	0.12	0.47
Decrease 0.05 - 0.1	0.90	1.07	0.76	2.04
Decrease 0.05 - 0.025	1.44	3.26	1.30	5.51
Neutral -0.025 to +0.025	43.66	40.00	52.60	45.64
Increase 0.025 - 0.05	40.48	23.55	29.84	21.82
Increase 0.05 - 0.1	11.92	28.70	14.68	20.10
Increase > 0.1	1.43	3.25	0.70	4.42
Total	100	100	100	100

Table 1. Changes in Raw NDVI for the study area[1]

[1]Percent of pixels which fall into each of the change categories for each of the time periods.

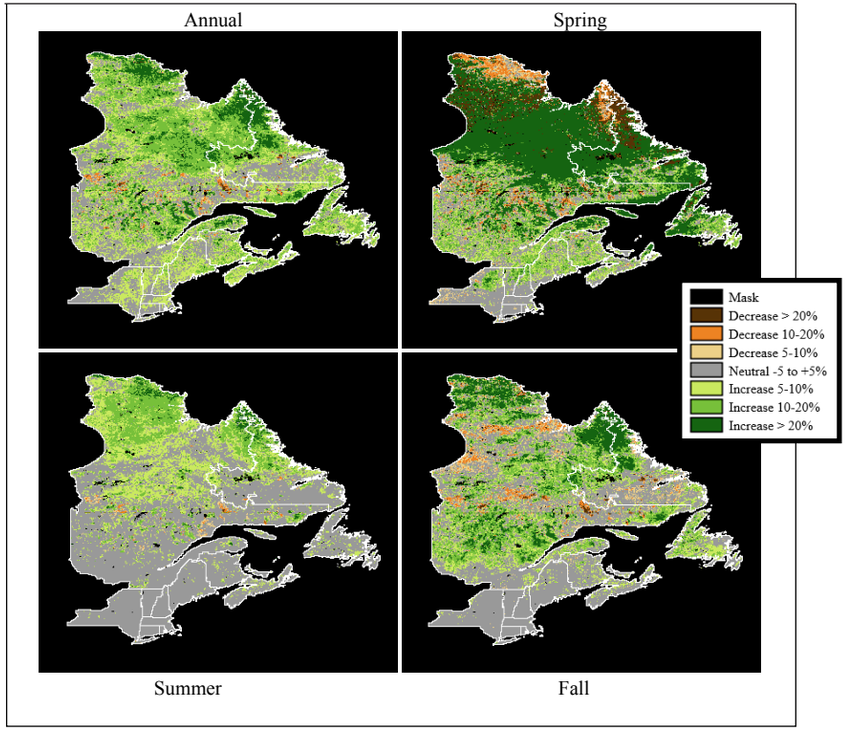

Figure 4. Percent change in NDVI: Total Study Area.

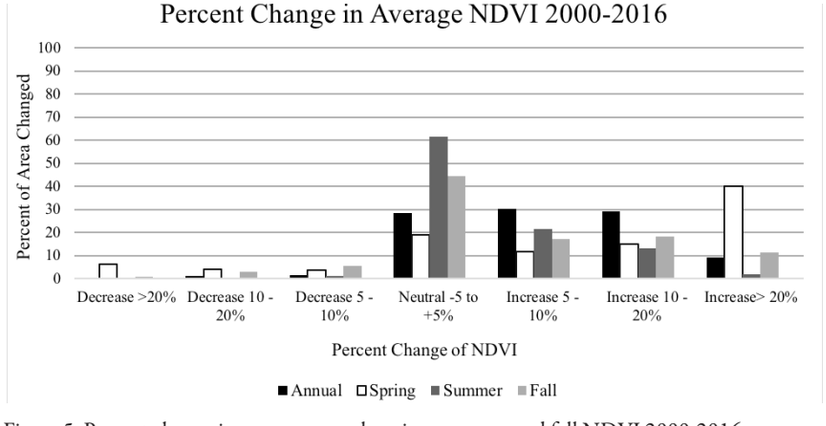

Figure 5. Percent change in average annual, spring, summer and fall NDVI 2000-2016.

Change of Average NDVI for Total Area-Percent Change				
Percent Change	Annual	Spring	Summer	Fall
Decrease > 20%	0.37	6.41	0.03	0.62
Decrease 10 - 20%	1.13	4.09	0.42	2.84
Decrease 5 - 10%	1.48	3.58	1.10	5.44
Neutral -5 to +5%	28.47	19.16	61.62	44.52
Increase 5 - 10%	30.24	11.84	21.59	17.14
Increase 10 - 20%	29.31	14.91	13.21	18.18
Increase > 20%	9.00	40.01	2.03	11.27
Total	100	100	100	100

Table 2. Percent of pixels which fall into each of the change categories for each of the time periods[1]

[1]Percent of pixels which fall into each of the change categories for each of the time periods.

level of agreement with 99.9 percent of the NDVI pixels increasing greater than 0.1 were also significant, while the lowest level of agreement was in the spring with 84.7 percent (Table 4). Pixels of decreasing NDVI were not as closely related with the pixels of significant change where those pixels decreasing in NDVI more than 0.1 had a similarity percent ranging from 35.3 percent (fall) to 78.7 percent (spring).

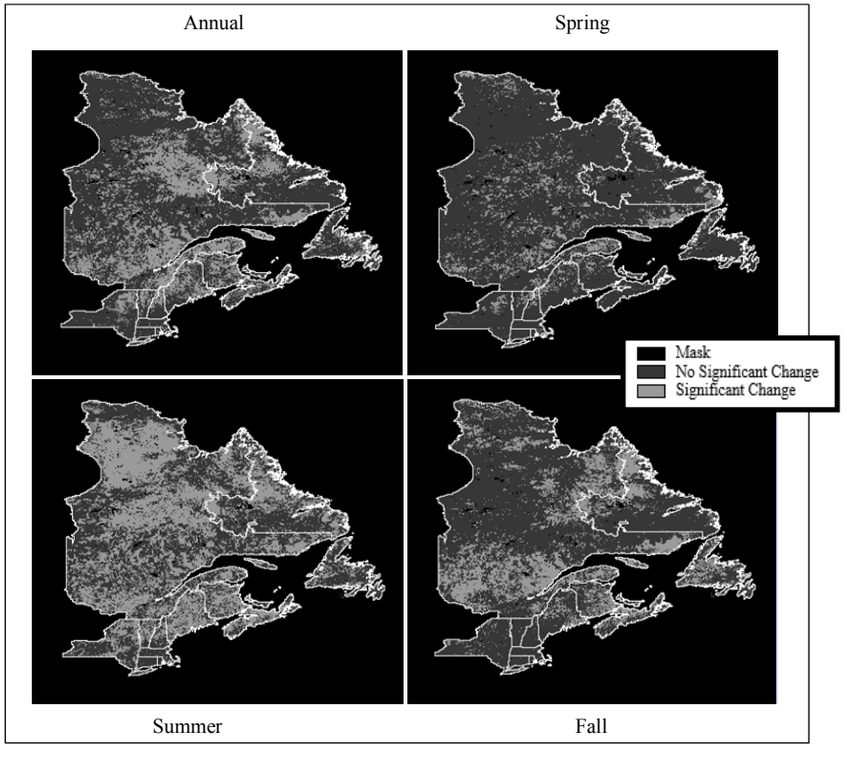

Figure 6. Depicts areas of significant change.

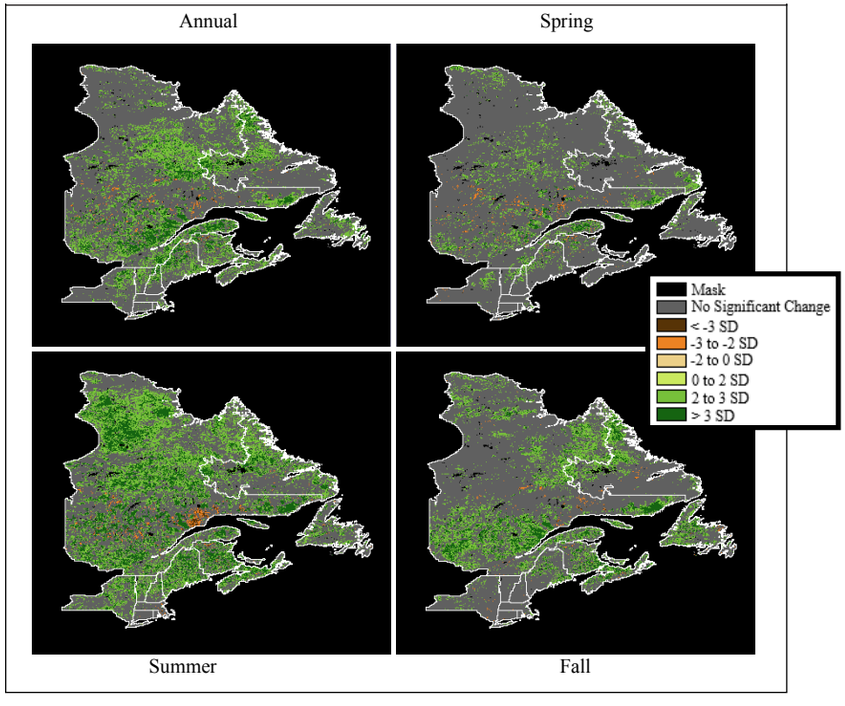

Figure 7. Depicts the areas of significant NDVI increase and areas of Significant NDVI decrease.

Percent of Area to Experience Change				
Intensity of Change	Annual	Spring	Summer	Fall
No Significant Change	69.16	88.20	50.74	73.34
<-3 SD	0.10	0.09	0.34	0.06
-3 to -2 SD	0.66	0.75	1.05	0.51
-2 to 0 SD	0.00	0.00	0.01	0.00
0 to 2 SD	0.03	0.09	0.15	0.08
2 to 3 SD	22.37	9.09	30.38	19.03
>3 SD	7.68	1.77	17.34	6.98
Total	100	100	100	100

Table 3. Percent and intensity of significant change at the 95% confidence level[1]

[1]Percent of pixels which fall into each of the change categories for each of the time periods.

Percent of Significant Raw Difference				
Change in NDVI	Annual	Spring	Summer	Fall
<-0.1	55.0	78.7	44.1	35.3
-0.1 to -0.05	43.6	45.6	46.8	10.5
-0.05 to -0.025	46.6	6.2	42.8	2.0
-0.025 to 0.025	3.7	3.4	24.8	4.1
0.025 to 0.05	42.2	8.0	74.1	3.4
0.05 to 0.1	83.6	2.0	84.9	63.5
>0.1	99.9	84.7	94.5	92.7

Table 4. The percent of the raw NDVI change that was determined to be significant at the 95% confidence level.1

[1]Values here indicate, of the Raw Difference pixels found in each category what percent of them were also significant at the 95% confidence level.

MOD13C2 NDVI Profiles

The NDVI profiles show annual and seasonal yearly NDVI averages for the entire 17-year study period along with a 3-year running average (Figure 8). The annual data graph in Figure 8 depicts the average NDVI for the entire study area for each year between 2000 and 2016, and displays an increase in the average NDVI from 0.3689 to 0.4029. This is a 0.034 increase over the seventeen years. The yearly spring average NDVI (months March, April and May) graph displays the greatest level of inter-annual variation in NDVI over the study period. These fluctuations may in part be caused by variations in snow coverage, which hinders the collection of NDVI data. Despite these extreme fluctuations, a general increase in the average spring NDVI is seen, as it increases from 0.2166 to 0.2449. The yearly summer average NDVI (months of June, July and August) graph displays a steadier increase in the average NDVI and also exhibits the largest increase in the average NDVI over the 17-year period. The yearly fall average NDVI (September, October and November) displays several fluctuations in NDVI as well with one particularly steep drop in 2002. Despite this decrease, the average NDVI for the fall season still displays a modest increase of 0.0095.

Changes in Land Cover and Total Study Area

Changes in the eight major land cover types were analyzed using the MODIS MCD12C1 land cover product (Figure 9). The total study area and the eight land covers were analyzed for changes in NDVI that were significant at the 95 percent confidence level. Table 5 shows the percent of the study area and each cover type that experienced significant change at the annual and seasonal scales. While the study area and all the cover types did experience some significant change, the percent of area impacted by change varies greatly across the seasons. For example,

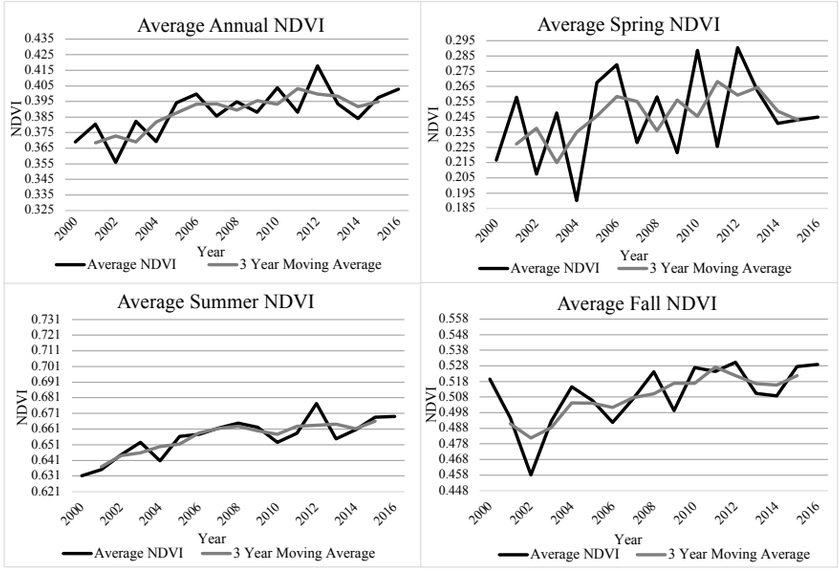

Figure 8. NDVI Profiles. The NDVI profiles show inter-annual variation throughout the entire 17-year period at the annual, spring (March, April, May), summer (June, July, August) and fall (September, October, November) scales. An increase in the average yearly NDVI can be seen at all scales.

the total study area experienced little change during the spring (11.8 percent) while during the summer; almost half of the area was impacted by significant change. However, at the annual level, only about 30 percent of the area experienced change. The savannas, open shrub lands and mixed forest all experienced significant change during the summer ranging from 48 to 63.51 percent of the given area. Yet only 9 to 18.27 percent of those same cover types experienced change during the spring. The mixed forest is notable as almost half of this cover type experienced significant change at the annual scale and more than 50 percent during the summer. The mixed forest experienced the largest amount of significant change of the eight cover types, at the annual scale. The open shrub lands experienced the greatest seasonal change with 63.5 percent in the summer. In comparison,

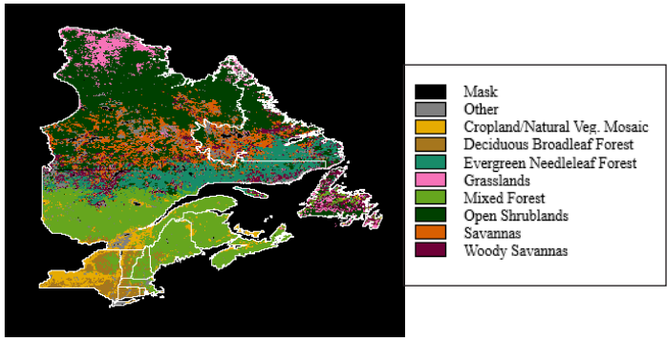

Figure 9. The eight largest landcover types within the study area.

Percent of Land Cover Area to Experience Significant Change				
	Percent of Area			
Land Cover Type	Annual	Spring	Summer	Fall
Total Study Area	30.84	11.80	49.26	26.66
Cropland & Natural Veg. Mosaic	20.68	6.14	42.67	23.73
Deciduous Broadleaf Forest	29.21	11.03	39.02	3.91
Evergreen Needleleaf Forest	16.21	12.08	34.44	18.90
Grasslands	19.71	14.48	37.33	22.95
Mixed Forest	48.35	18.27	52.95	44.47
Open Shrublands	30.46	9.33	63.51	25.54
Savanna	30.00	9.53	48.15	17.33
Woody Savanna	24.61	10.53	32.86	24.72

Table 5. The percent of area that experienced change significant at the 95% confidence level, regardless of the direction of change

the evergreen needleleaf forest experienced the least amount of significant change at the annual scale, only 16.21 percent of the area.

When looking at the intensity and direction of the change for the overall study area (Table 3) and within each cover type (Tables 6A-H), it should be noted that, though they are small, there were some areas of significant NDVI decrease. These areas of significant decrease can be seen across the total study area and within each of the cover types at all scales. The evergreen needleleaf forest experienced the largest decrease in NDVI at the annual, spring, and summer scales. A total of 3.67 percent, 3.87 percent, and 6.70 percent of the area, respectively, experienced a decrease in NDVI, much of which was by more than two standard deviations. The majority of change seen in the total study area and within each cover types however is positive at all scales, reflecting a significant increase in NDVI at the 95 percent confidence level. Increases in NDVI during the spring season are among the smallest seen, ranging from 5.74 percent to 17.12 percent of the area. Again, the mixed forest and open shrub lands are notable as more than half of each cover type experienced significant positive change at the summer scale, 50.83 percent and 53.48 percent respectively (Tables 6E and F). Most of this change is more than two standard deviations from the mean. The mixed forest also had the largest increase at the annual and the fall scales where, respectively, 47.43 percent and 43.99 percent of the area increased in NDVI by more than two standard deviations. The evergreen needleleaf forest experienced the smallest increase at the annual scale, only 12.54 percent of the area increased in NDVI.

Table 6A-H. These tables show the percent of area to experience significant change, along with the direction and intensity of change for each of the eight land cover types.

Cropland & Nat. Veg	Percent of area to Experience Change			
Intensity of Change	Annual	Spring	Summer	Fall
No Significant Change	79.32	93.86	57.33	76.27
<-3 SD	0.00	0.02	0.10	0.00
-3 to -2 SD	0.02	0.36	0.33	0.55
-2 to 0 SD	0.00	0.02	0.00	0.02
0 to 2 SD	0.02	0.00	0.17	0.10
2 to 3 SD	14.96	4.39	27.90	15.41
> 3 SD	5.69	1.35	14.16	7.64

Table 6A.

Deciduous Broadleaf	Percent of area to Experience Change			
Intensity of Change	Annual	Spring	Summer	Fall
No Significant Change	70.79	88.97	60.98	96.09
<-3 SD	0.00	0.00	0.02	0.02
-3 to -2 SD	0.00	0.10	0.22	0.38
-2 to 0 SD	0.00	0.00	0.00	0.02
0 to 2 SD	0.10	0.07	0.34	0.02
2 to 3 SD	22.90	9.64	27.77	3.31
> 3 SD	6.21	1.22	10.67	0.14

Table 6B.

Evergreen Needleleaf	Percent of area to Experience Change			
Intensity of Change	Annual	Spring	Summer	Fall
No Significant Change	83.79	87.92	65.56	81.10
<-3 SD	0.47	0.42	2.30	0.27
-3 to -2 SD	3.20	3.43	4.36	1.47
-2 to 0 SD	0.00	0.02	0.03	0.01
0 to 2 SD	0.02	0.01	0.10	0.01
2 to 3 SD	9.65	7.02	15.91	12.17
> 3 SD	2.86	1.18	11.74	4.98

Table 6C

Grasslands	Percent of area to Experience Change			
Intensity of Change	Annual	Spring	Summer	Fall
No Significant Change	80.29	85.52	64.27	77.05
<-3 SD	0.02	0.00	0.00	0.00
-3 to -2 SD	0.03	0.00	0.00	0.24
-2 to 0 SD	0.00	0.00	0.00	0.00
0 to 2 SD	0.02	0.39	0.03	0.11
2 to 3 SD	16.19	12.62	26.11	18.71
> 3 SD	3.45	1.47	9.59	3.88

Table 6D

Mixed Forest	Percent of area to Experience Change			
Intensity of Change	Annual	Spring	Summer	Fall
No Significant Change	51.65	81.73	47.05	55.53
<-3 SD	0.15	0.14	0.37	0.08
-3 to -2 SD	0.78	1.01	1.74	0.39
-2 to 0 SD	0.00	0.00	0.01	0.00
0 to 2 SD	0.02	0.04	0.27	0.12
2 to 3 SD	30.38	13.17	28.37	28.96
> 3 SD	17.03	3.91	22.20	14.91

Table 6E

Open Shrubland	Percent of area to Experience Change			
Intensity of Change	Annual	Spring	Summer	Fall
No Significant Change	69.54	90.67	36.49	74.46
<-3 SD	0.00	0.01	0.00	0.01
-3 to -2 SD	0.04	0.04	0.03	0.16
-2 to 0 SD	0.00	0.00	0.00	0.00
0 to 2 SD	0.04	0.11	0.13	0.08
2 to 3 SD	24.14	8.09	41.24	19.95
> 3 SD	6.23	1.07	22.12	5.34

Table 6F

Savanna	Percent of area to Experience Change			
Intensity of Change	Annual	Spring	Summer	Fall
No Significant Change	70.00	90.47	51.85	82.67
<-3 SD	0.02	0.05	0.02	0.06
-3 to -2 SD	0.61	0.42	0.41	0.85
-2 to 0 SD	0.00	0.00	0.00	0.00
0 to 2 SD	0.03	0.06	0.09	0.07
2 to 3 SD	23.41	8.09	31.12	13.57
> 3 SD	5.92	0.90	16.50	2.77

Table 6G

Woody Savanna	Percent of area to Experience Change			
Intensity of Change	Annual	Spring	Summer	Fall
No Significant Change	75.39	89.47	67.14	75.28
<-3 SD	0.15	0.13	0.20	0.05
-3 to -2 SD	1.14	1.30	1.58	0.73
-2 to 0 SD	0.00	0.00	0.03	0.01
0 to 2 SD	0.03	0.03	0.11	0.08
2 to 3 SD	18.78	7.34	20.82	16.85
> 3 SD	4.51	1.73	10.12	7.00

Table 6H

Land Surface Temperature Change

Based on the analysis of the MOD11C3 LST data, it is clear that the northeastern region of North American has experienced an extensive warming between 2000 and 2016 (Table 7, Figures 10 and 11). Most of the increase in temperature occurred in the summer with more than 80 percent of the region increasing in temperature > 0.5° C while more than 35 percent of the study area increased > 0.5° C annually and during the fall. Although spring saw the smallest area of increase, still more than 30 percent increased greater than 0.5°C. Fall had the highest decrease with 6 percent decreasing more than 0.5° C. The temporal profiles of LST (Figure 11) graph the yearly average LST for all pixels in the study area for each season and at the annual scale. The linear trends for the LST temporal profiles show that the region increased in LST at each of the scales. The temperature profiles for all of the seasons and at the annual scale show considerable inter-annual variation, especially in the spring.

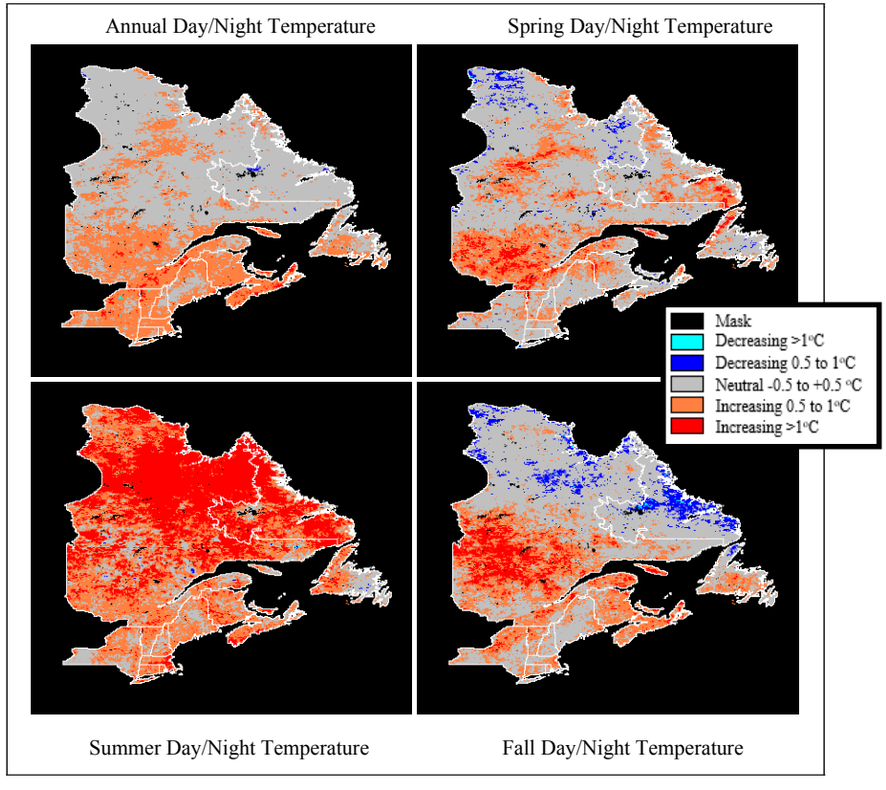

Figure 10. Images depicting the raw change in average land surface temperature at the annual, spring, summer and fall scales.

Change in Average Seasonal Day and Night Temperatures								
	Percent of Area							
	Annual		**Spring**		**Summer**		**Fall**	
Raw Change in Temp.	Day	Night	Day	Night	Day	Night	Day	Night
Decrease > 1 ºC	0.10	0.01	1.24	0.33	0.98	0.00	1.07	1.35
Decrease 0.5 to 1 ºC	0.94	0.25	6.14	4.36	2.20	0.01	6.55	9.82
Neutral -0.5 to + 0.5 ºC	70.80	52.97	55.37	64.52	32.42	8.81	52.64	55.94
Increase 0.5 to 1 ºC	24.51	39.35	24.13	25.28	30.98	31.59	24.88	25.26
Increase > 1 ºC	3.65	7.42	13.12	5.51	33.41	59.58	14.86	7.63

Table 7. Change in Annual and Seasonal Day and Night Temperatures.

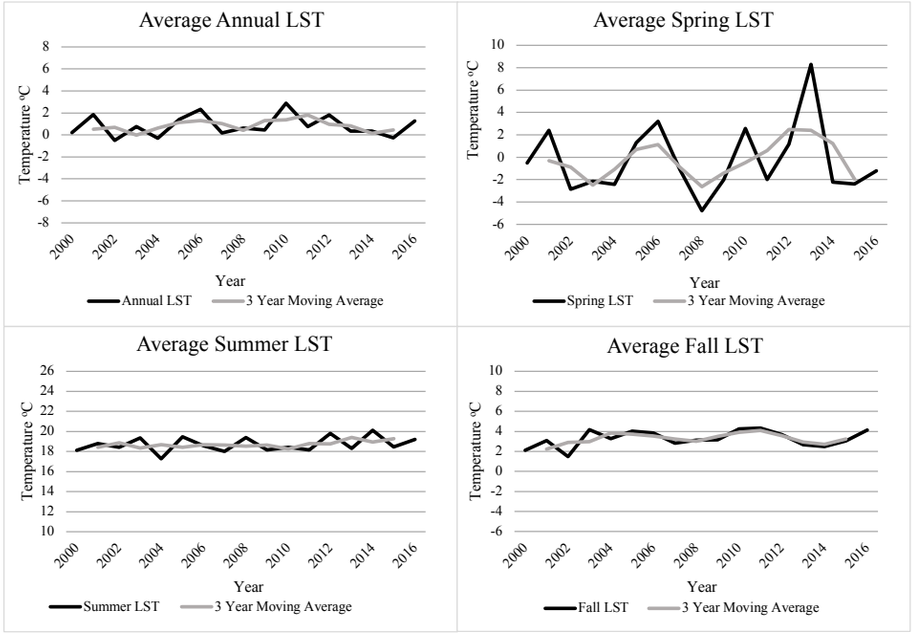

Figure 11. LST Profiles. The LST profiles show inter-annual variation throughout the entire 17-year period at the annual, spring (March, April, May), summer (June, July, August) and fall (September, October, November) scales.

To test the significance of the temperature change that we saw in the region we ran a Mann-Kendall statistic. The results (Table 8) show that most of the region experienced non-significant changes (95 percent confidence level) with summer experiencing the greatest significant change at 5 percent of the entire region. Not only did the region not experience a significant temperature change, the relationship between temperature change and NDVI change is very weak as indicated by a weak correlation coefficient between changing NDVI and changing temperature. A correlation coefficient near zero indicates an inverse relationship and a correlation coefficient of one indicates a pattern, which is identical. Correlation coefficients near 0.5 indicate little relationship between the two data sets. The correlation coefficient between changing temperature and NDVI for the entire time period was 0.634 at the annual level and 0.568 for the spring, 0.433 for the summer and 0.544 for the fall, all indicating not a close relationship.

Significant LST Simple Differencing Change				
Simple Differencing Change	Annual	Spring	Summer	Fall
Significant Change of entire area[1]	0.1	0.1	5.0	3.7
Decrease > 1 ^{0}C[2]	18	67	618	16
Decrease 1 to 0.5 ^{0}C	10	0	198	2
Neutral -0.5 to + 0.5 ^{0}C	0	0	46	8
Increase 0.5 to 1 ^{0}C	22	0	91	204
Increase > 1 ^{0}C	219	1	5065	4249

Table 8. The percent of Simple Differencing LST change that was determined to be significant at the 95% confidence level.

1. For the entire study area, what percent of LST Simple Differencing change pixels were found to be significant at the 95% confidence level.
2. Of the Simple Differencing change pixels in this category, what percent were found to be signifi cant at the 95% confidence level.

Discussion and Conclusion

The year 2016 was the warmest year in NOAA's 137-year temperature series. Not only was the average 2016 global temperature 0.94°C above the 20th century average, it was also the third consecutive year be labeled as the warmest year in the last 137 years of meteorological record-keeping (NOAA 2017). The world is warming, and we have observed this through land and ocean temperature measurements, the melting of sea-ice and glaciers, and the thermal expansion of seas. We are also observing a greening of the high northern latitudes. This research shows that northeast North America is no exception and that between 2000 and 2016 we have observed significant increases in photosynthesis as captured by satellites through NDVI measurements.

Although the smallest increases in NDVI were during the spring, much of the considerable increases in NDVI can be seen in the summer throughout the study area. A substantial increase in NDVI can be seen at the annual and fall scales as well. The most notable and most intense greening is occurring in the higher latitudes where the open shrub lands are located, and in the lower latitudes where the mixed forests are located. Decreases in spring snow cover have also been noted which might be allowing vegetation to grow more vigorously in the spring season (Choi, Robinson, and Kang 2010). Similar observations have been made in many parts of the high northern latitudes indicating an earlier start to the spring growing season (Shen et at. 2014). The open shrub lands (located in the northern latitudes of the study area) have increased slightly in NDVI during the spring and display greater increases in during the summer and fall seasons.

Though the bulk of the study area remains unchanged at each of the seasonal and annual scales, there is a notable increase in NDVI. At the annual scale (which consists of the average NDVI for all seasons, including winter) almost a third of the study area does display an increase

in greening of vegetation, with 30.09 percent of the area increasing in NDVI. When looking at the seasons, the summer displays the greatest increase, where 47.87 percent of the study area increased in NDVI. Some of the most intense increases occurred during the summer in the open shrub lands (northern latitudes) and mixed forest (lower latitudes) where over 63 percent and 50 percent of the land cover increased in NDVI respectively. The open shrub lands and mixed forests continued to increase in NDVI during the fall as well. In contrast, 26.09 percent of the study area increased in NDVI during the fall.

Like the greening of the region, the temperature of the land surface also increases extensively. The summer season saw the greatest increase of LST with over 84 percent of the region warming greater than 0.5° C and more than 42 percent of the area warming greater than 1° C. During the spring and fall, the central and southern portions of the region warmed while the more northern areas remained unchanged and a few locations in the north cooled as well. Despite much of the region experiencing an increase of LST greater than 0.5° C, based on our Mann-Kendall statistics, there was not an extensive significant (95 percent confidence level) increase in LST. Other than during the summer, there was not a strong relationship between the land surfaces warming and regions increasing in NDVI. Near surface air temperature (meteorological temperatures) and the temperatures of the surface of the earth (derived from satellites) are related but are different from each other (Vancutsem et al. 2010). The near surface air temperatures can be increasing while the surface temperatures are not. One factor that can influence the land surface temperature is vegetation where increases in vegetation can decrease the temperature of the surface of the earth (Kaufmann et al. 2003) and this factor maybe why the LST and NDVI data sets are not as correlated as one might expect with a warming world. There is no doubt, however, that based on our research the northeastern part of North America is increasing extensively in both land surface temperature and photosynthesis between 2000 and 2016.

Kristen Thiebault is a graduate of Salem State University where she earned her Masters of Science in Geo-Information Science. Her research interests include climate change and conservation. E-mail: kristen.m.thiebault@gmail.com

Stephen Young is a professor in the Department of Geography at Salem State University and his research focuses on using remote sensing to analyze environmental change. Email: syoung@salemstate.edu

Acknowledgements

We would like to take a moment to thank: NASA Land Processes Distributed Active Archive Center for use of the MODIS LST and NDVI data, the University of Maryland Global Land Cover Facility for the use of the land cover map, the two anonymous reviewers for their extensive comments, and the editor of the journal for comments and assistance on the article.

References

Andela, N. and G. R. Van Der Werf. 2014. Recent trends in African fires driven by cropland expansion and El Niño to La Niña transition. *Nature Climate Change* 4 (9): 791.

Bastos, A., P. Ciais, T. Park, J. Zscheischler, C. Yue, J. Barichivich, R. B. Myneni, S. Peng, S. Piao, and S. Zhu. 2017. Was the extreme northern hemisphere greening in 2015 predictable?. *Environmental Research Letters* 12 (4): 044016.

Bhatt, U. S., D. A. Walker, M. K. Raynolds, J. C. Comiso, H. E. Epstein, G. Jia, R. Gens, J. E. Pinzon, C. J. Tucker, C. E. Tweedie, and P. J. Webber. 2010. Circumpolar Arctic tundra vegetation change is linked to sea ice decline. *Earth Interactions* 14 (8): 1-20.

Chen, I. C., J. K. Hill, R. Ohlemüller, D. B. Roy, and C. D. Thomas. 2011. Rapid range shifts of species associated with high levels of climate warming. *Science* 333 (6045): 1024-1026.

Chen, J. M., B. Chen, K. Higuchi, J. Liu, D. Chan, D. Worthy, P. Tans, and A. Black. 2006. Boreal ecosystems sequestered more carbon in warmer years. *Geophysical Research Letters* 33 (10).

Choi, G., D. A. Robinson, and S. Kang. 2010. Changing northern hemisphere snow seasons. *Journal of Climate* 23 (19): 5305-5310.

Clark University. 2015. TerrSet Geospatial Monitoring and Modeling Software. https://clarklabs.org/terrset/ (last accessed 8 September 2016).

Detsch, F., I. Otte, T. Appelhans, and T. Nauss. 2016. A comparative study of cross-product NDVI dynamics in the Kilimanjaro region—A matter of sensor, degradation, calibration, and significance. *Remote Sensing* 8 (2): 159.

Didan, K., A. B. Munoz, R. Solano, and A. Huete. 2015. *MODIS Vegetation Index User's Guide* (MOD13 Series). Version 3.00, Collection 6. June 2015. PDF.

Didan, K. 2015. MOD13C2 MODIS/Terra Vegetation Indices Monthly L3 Global 0.05Deg CMG V006. NASA EOSDIS Land Processes DAAC. doi: 10.5067/MODIS/MOD13C2.006.

Duarte, C. M., Lenton, T. M., Wadhams, P. and P. Wassmann. 2012. Abrupt climate change in the Arctic. *Nature Climate Change* 2 (2): 60-62.

Elmendorf, S. C., G. H. Henry, R. D. Hollister, R. G. Björk, N. Boulanger-Lapointe, E. J. Cooper, J. H. Cornelissen, T. A. Day, E. Dorrepaal, T. G. Elumeeva, M. Gill, W. A. Gould, J. Harte, D. S. Hik, A. Hofgaard, D. R. Johnson, J. F. Johnstone, I. S. Jonsdottir, J. C. Jorgenson, K, Klanderud, J. A. Klein, A. Koh, G. Kudo, M. Lara, E. Levesque, B. Magnusson, J. L. May, J. A. Mercado-Di'az, A. Michelsen, U. Molau, I. H. Myers-Smith, S. F. Oberbauer, V. G. Onipchenko, C. Rixen, N. M. Schmidt, G. R. Shaver, M. J. Spasojevic, Þ. E. Þórhallsdóttir, A. Tolvanen, T. Troxler, C. E. Tweedie, , S. Villareal, C.-H. Wahren, X. Walker, P. J. Webber, M. J. Welker, and S. Wipf. 2012. Plot-scale evidence of tundra vegetation change and links to recent summer warming. *Nature Climate Change*, 2 (6): 453-7.

Fraser, R. H., I. Olthof, M. Carrière, A. Deschamps, and D. Pouliot. 2011. Detecting long-term changes to vegetation in northern Canada using the Landsat satellite image archive. *Environmental Research Letters* 6 (4): 045502.

Friedl, M. A., D. Sulla-Menashe, B. Tan, A. Schneider, N. Ramankutty, A. Sibley, and X. Huang. 2010. MODIS Collection 5 global land cover: Algorithm refinements and characterization of new datasets. *Remote Sensing of Environment*, 114 (1): 168–182.

Gaddam, V.K., P. Sharma, L.K. Patel, T. Meloth, and A. Singh. 2016. Analysis of spatio-temporal variations in snow cover over western Himalaya. *In Proceedings of SPIE Vol. 9877: Land Surface and Cryosphere Remote Sensing III*, ed. R. Khanbilvardu, A. Gangu, A. S. Rajawat, and J. M. Chen. 98772A. Bellingham WA: SPIE.

Hansen, J. E. and M. Sato. 2012. Paleoclimate implications for human-made climate change. In *Change: Inferenced from paleoclimate and regional aspects*, ed. A. Berger, F. Mesinger, and D. Šijački 21-48. Vienna, Austria: Springer.

Hansen, M. C., P. V. Potapov, R. Moore, M. Hancher, S. A. Turubanova, A. Tyukavina, D. Thau, S. V. Stehman, S. J. Goetz, T. R. Loveland, and A. Kommareddy. 2013. High-resolution global maps of 21st-century forest cover change. *Science* 342 (6160): 850-853.

Jiménez-Muñoz, J. C., J. A. Sobrino, C. Mattar, and Y. Malhi. 2012. Multi-temporal analysis of MODIS land products over the Amazon region. In *Proceedings of 2012 IEEE International Geoscience and Remote Sensing Symposium*. 6439-6442. IEEE.

Ju, J. and J. G. Masek. 2016. The vegetation greenness trend in Canada and U.S. Alaska from 1984–2012 Landsat data. *Remote Sensing of Environment* 176: 1-16.

Kafatos, M. 2007. The cooling effect of vegetation on LST is stronger during daytime than nighttime. Sun, DL and GEOPHYSICAL RESEARCH LETTERS, 34: L24406, doi: 10.1029/2007GL031485.

Kaufmann, R. K., L. Zhou, R. B Myneni, C. J. Tucker, D. Slayback, N. V. Shabanov, and J. Pinzon. 2003. The effect of vegetation on surface temperature: A statistical analysis of NDVI and climate data. *Geophysical Research Letters* 30 (22): 2147.

Kimball, J. S., L. A. Jones, K. Zhang, F. A. Heinsch, K. C. McDonald, and W. C. Oechel. 2009. A satellite approach to estimate land–atmosphere exchange for boreal and Arctic biomes using MODIS and AMSR-E. *IEEE Transactions on Geoscience and Remote Sensing* 47 (2): 569-587.

Kumar, P. and C. Jeganathan, 2017. Monitoring Horizontal and Vertical Cropping Pattern and Dynamics in Bihar over a Decade (2001–2012) Based on Time-Series Satellite Data. *Journal of the Indian Society of Remote Sensing* 45 (3): 485-502.

McGuire, A. D., Anderson, L. G., Christensen, T. R., Dallimore, S., Guo, L., Hayes, D. J., Heimann, M., Lorenson, T. D., Macdonald, R. W. and N. Roulet. 2009. Sensitivity of the carbon cycle in the Arctic to climate change. *Ecological Monographs* 79 (4): 523-555.

Menzel, A., T. H. Sparks, N. Estrella, E. Koch, A. Aasa, R. Ahas, A. Zust. 2006. European phenological response to climate change matches the warming pattern. *Global Change Biology* 12: 1969–1976.

Mildrexler, D., M. Zhao, F. Heinsch, and S. Running. 2007. A new satellite-based methodology for continental-scale disturbance detection. *Ecological Applications* 17 (1): 235-50.

NASA. (n.d.). Reverb Echo: The next generation Earth science discovery tool. http://reverb.echo.nasa.gov/reverb. (last accessed 8 September 2016).

Neeti, N. and R. Eastman. 2011. A contextual Mann-Kendall approach for the assessment of trend significance in image time series. *Transactions in GIS* 15 (5): 599-611.

NOAA. 2017. National Centers for Environmental Information. State of the Climate: Global Analysis for Annual 2016. http://www.ncdc.noaa.gov/sotc/global/201613. (last accessed 12 March 2017).

Parmesan, C. 2006. Ecological and evolutionary responses to recent climate change. *Annual Review of Ecology, Evolution, and Systematics* 37 (2006): 637-669.

Peng, C., Z. Ma, X. Lei, Q. Zhu, H. Chen, W. Wang, S. Liu, W. Li, X. Fang, and X. Zhou. 2011. A drought-induced pervasive increase in tree mortality across Canada's boreal forests. *Nature Climate Change* 1 (9): 467-471.

Pouliot, D., R. Latifovic, and I. Olthof. 2009. Trends in vegetation NDVI from 1 km AVHRR data over Canada for the period 1985–2006. *International Journal of Remote Sensing* 30 (1): 149-168.

Ren, G., S. S. Young, L. Wang, W. Wang, Y. Long, R. Wu, J. Li, J. Zhu, and D. W. Yu. 2015. Effectiveness of China's national forest protection program and nature reserves. *Conservation Biology* 29 (5): 1368-1377.

Schlaepfer, D. R., W. K. Lauenroth, and J. B. Bradford. 2012. Consequences of declining snow accumulation for water balance of mid-latitude dry regions. *Global Change Biology* 18 (6): 1988-1997.

Schuur, E. A. G., A. D. McGuire, C. Schädel, G. Grosse, J. W. Harden, D. J. Hayes, G. Hugelius, C. D. Koven, P. Kuhry, D. M. Lawrence, and S. M. Natali. 2015. Climate change and the permafrost carbon feedback. *Nature* 520 (7546): 171-179.

Serreze, M. C. and J. A. Francis. 2006. The Arctic amplification debate. *Climatic Change* 76 (3-4): 241-264.

Shen, M., Y. Tang, J. Chen, X. Yang, C. Wang, X. Cui. Y. Yang, L. Han, L. Li, J. Du, G. Zhang, and N. Cong. 2014. Earlier-season vegetation has greater temperature sensitivity of spring phenology in northern hemisphere. PLoS ONE 9 (2): e88178. doi: 10.1371/journal.pone.0088178.

Singh, A. 1989. Review article digital change detection techniques using remotely-sensed data. *International Journal of Remote Sensing* 10 (6): 989-1003.

Tape, K. E. N., M. Sturm, and C. Racine. 2006. The evidence for shrub expansion in northern Alaska and the Pan-Arctic. *Global Change Biology* 12 (4): 686-702.

Takebayashi, H., and M. Moriyama. 2007. Surface heat budget on green roof and high reflection roof for mitigation of urban heat island. *Building and Environment* 42 (8): 2971-2979.

Vancutsem, C., P. Ceccato, T. Dinku, and S. J. Connor. 2010. Evaluation of MODIS land surface temperature data to estimate air temperature in different ecosystems over Africa. *Remote Sensing of Environment* 114 (2): 449-465.

Wan, Z., 2013. Collection-6 MODIS land surface temperature products users' guide. *ICESS, University of California, Santa Barbara*.

———, 2014. New refinements and validation of the collection-6 MODIS land-surface temperature/emissivity product. *Remote sensing of Environment* 140 (2014): 36-45.

Wang, L., S. S. Young, W. Wang, G. P. Ren, W. Xiao, Y. C. Long, J. S. Li, and J. G. Zhu. 2016. Conservation priorities of forest ecosystems with evaluations of connectivity and future threats: Implications in the eastern Himalaya of China. *Biological Conservation* 195: 128-135.

Xie, Y., Z. Sha, and M. Yu. 2008. Remote sensing imagery in vegetation mapping: a review. *Journal of Plant Ecology* 1 (1): 9-23.

Yi, Y., J. S. Kimball, L. A. Jones, R. H. Reichle, R. Nemani, and H. A. Margolis. 2013. Recent climate and fire disturbance impacts on boreal and arctic ecosystem productivity estimated using a satellite-based terrestrial carbon flux model. *Journal of Geophysical Research: Biogeosciences* 118 (2): 606-622.

Young, S. S.. 2004. Satellite detected broad-scale vegetation change in China, 1982 – 1999. *Asian Geographer* 22 (1-2): 123-142.

Young, S. S. and R. Harris. 2005. Changing patterns of global-scale vegetation photosynthesis, 1982–1999. *International Journal of Remote Sensing* 26 (20): 4537-4563.

Yu, W., M. Ma, X. Wang, L. Geng, J. Tan, and J. Shi. 2014. Evaluation of MODIS LST products using longwave radiation ground measurements in the northern arid region of China. *Remote Sensing* 6 (11): 11494-11517.

Zhang, K., J. S. Kimball, E. H. Hogg, M. Zhao, W. C. Oechel, J. J. Cassano, and S. W. Running. 2008. Satellite-based model detection of recent climate-driven changes in northern high-latitude vegetation productivity. Journal of Geophysical Research: *Biogeosciences*, 113 (G3).

Zhang, X., M. A. Friedl, C. B. Schaaf, and A. H. Strahler. 2004. Climate controls on vegetation phenological patterns in northern mid-and high latitudes inferred from MODIS data. *Global Change Biology* 10 (7): 1133-1145.

INFLUENCE OF LAKE MORPHOMETRY

On Paleoproductivity Patterns in Lakes Subjected to Similar Climate Change Conditions in the Adirondack Mountains of New York, Eastern North America

Sarah Robinson
Utica College

Sharon L. Kanfoush
Utica College

ABSTRACT

Several published studies reported geographically proximal lakes subjected to similar climatic conditions responded similarly. In the Fulton Chain of Lakes, one study reported changes in diatoms of one of the lakes, Fourth Lake, correlated with changes in northern hemisphere temperature (NH-T), atmospheric CO_2, and solar irradiance. Subsequent research, however, found other lakes in the chain, each proximate and hydrologically-connected, did not exhibit synchrony in changes in physical and chemical sediment characteristics, due to differences in individual lake morphometry. We hypothesize the lakes' paleoproductivity also responded asynchronously. Old Forge Pond, Second Lake, and Third Lake of the chain were analyzed in this study. Although semi-connected and subjected to similar climate, these lakes possess varied morphometry. Short (28-31cm) mud-water interface cores recovered in 2006 were sampled every 1-cm, ^{210}Pb dated, and ≥400 diatom valves counted in each at 400x magnification.

Diatom concentration and accumulation in Old Forge Pond and Third Lake did not respond significantly to changes in NH-T, atmospheric CO_2, or solar irradiance. However, in Second Lake, diatom concentration correlates weakly with NH-T and strongly with atmospheric CO_2 (R = 0.28 and 0.66, respectively) and diatom accumulation with NH-T, CO_2, and irradiance (R = 0.58, 0.61, and 0.50, respectively). Positive correlations with these parameters are also observed for Second Lake % organics (R = 0.84, 0.91, and 0.56) and organics (g) (R = 0.54, 0.67, and 0.30). Thus, it appears productivity of these semi-connected lakes does not respond to climate forcing in a similar manner. Alternatively, some lakes may respond more substantially to land use changes. *Key words: climate change, diatoms, lake morphometry, paleoproductivity, synchrony.*

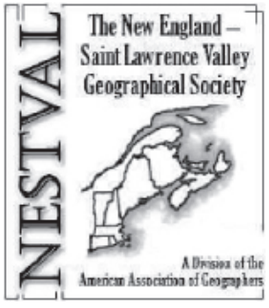

THE NEW ENGLAND-ST. LAWRENCE VALLEY GEOGRAPHICAL SOCIETY (NESTVAL) was founded in 1922 to promote scholarly research and disseminate geographic information in the region. Originally founded as the New England Geographical Conference, the current name was adopted in 1956. NESTVAL, one of nine regional divisions of the Association of American Geographers, sponsors an annual conference every fall that is open to members and non-members. Membership, which includes a subscription to the Journal, may be arranged with NESTVAL's Secretary-Treasurer (www.nestvalonline.org)

The Northeastern Geographer is an annual publication that replaces the *Proceedings of the New England-St. Lawrence Valley Geographical Society*. The *Proceedings* were published from 1972 until 2006. *The Northeastern Geographer* publishes research articles, essays and book reviews on all geographical topics but the focus of the Journal is on the Northeast United States, the St. Lawrence Valley and the Canadian Maritime Provinces. All research articles submitted to the Journal undergo peer-review.

The Northeastern Geographer

Journal of The New England-St. Lawrence Valley Geographical Society

Special Issue: Climate Change

VOLUME 9, 2017

Edited by

Steven E. Silvern,
Department of Geography, Salem State University
Email: negeog@salemstate.edu

Published by the New England-St. Lawrence Valley Geographical Society
(www.nestvalonline.org)